

Deformation Behavior and Workability of Supercooled Liquid in Zr₆₅Al₁₀Ni₁₀Cu₁₅ Metallic Glass

著者	KAWAMURA Yoshihito, SHIBATA Tsutomu, INOUE Akihisa
journal or publication title	Science reports of the Research Institutes, Tohoku University. Ser. A, Physics, chemistry and metallurgy
volume	43
number	2
page range	107-113
year	1997-03-25
URL	http://hdl.handle.net/10097/28661

Deformation Behavior and Workability of Supercooled Liquid in $Zr_{65}Al_{10}Ni_{10}Cu_{15}$ Metallic Glass*

Yoshihito KAWAMURA, Tsutomu SHIBATA and Akihisa INOUE

Institute for Materials Research, Tohoku University, Sendai 980-77, JAPAN

(Received January 30, 1997)

The tensile deformation behavior and the workability of $Zr_{65}Al_{10}Ni_{10}Cu_{15}$ Metallic Glass with a wide supercooled liquid have been examined. The glassy solid exhibited the homogeneous deformation at higher temperatures and lower strain rates. The supercooled liquid revealed a homogeneous deformation even at high strain rates above 0.5 s^{-1} . The strength in the homogeneous deformation region was lower at higher temperatures and lower strain rates. The supercooled liquid exhibited similar deformation behavior to the other high-strain-rate superplastic materials. Using this superplastic-like deformation in the supercooled liquid, complex-shaped glassy component with original strength was produced through an extrusion process.

KEYWORDS: $Zr_{65}Al_{10}Ni_{10}Cu_{15}$, amorphous, supercooled liquid, mechanical property, superplasticity

1. Introduction

It is well known that the mechanical properties of metallic glasses are essentially different from those of organic glasses^{1, 2)}. Glassy metals have a ductile nature enough to be bent through 180 degrees without fracture and can be rolled at a reduction ratio of about 50 % at room temperature. At low temperatures below about 100 K of the crystallization or glass-transition temperature, the glassy alloys usually exhibit an inhomogeneous deformation which is localized in discrete and thin shear bands, resulting from its nonhardenable nature. On the contrary, higher temperatures lead to a homogeneous deformation at strain rates below 10^{-3} s^{-1} . In this homogeneous deformation region, each volume element of the material contributes to strain, resulting in a uniform deformation for a uniformly stressed specimen. However, the elongation on tensile testing is limited to below 100 % and the strength is more than several tens percentages of the room-temperature strength, which are insufficient to hot-work the glassy alloys industrially. Recently, a number of glassy alloys with a wide supercooled liquid region above 60 K and high glass-forming ability have been discovered³⁻⁷⁾. These glassy alloys promise to allow the production of large-scale bulk glassy materials by consolidation of glassy powders^{8,9)} and casting at low cooling rates³⁻⁷⁾. Availability of the glassy alloys with a wide supercooled liquid region enables unique approaches for shaping and forming into complex-shaped components through significant viscous flow inherent to the supercooled liquid¹⁰⁾.

We have been investigating the mechanical properties of the glassy solid and supercooled liquid in a

$Zr_{65}Al_{10}Ni_{10}Cu_{15}$ glassy alloy with a significant supercooled liquid region of 105 K¹¹⁾. This metallic glass exhibits an excellent thermal stability which enables the measurement of many properties in the supercooled liquid state. In this paper, we report the deformation behavior and workability of the $Zr_{65}Al_{10}Ni_{10}Cu_{15}$ (at.%) glassy alloy.

2. Experimental Procedure

Alloy ingots were prepared by arc melting pure metals in a purified argon atmosphere. $Zr_{65}Al_{10}Ni_{10}Cu_{15}$ (at.%) glassy alloy ribbon with a cross section of about $1.0 \times 0.02 \text{ mm}^2$ was produced by a single-roller melt-spinning method in an argon atmosphere. The formation of a single glassy phase was confirmed by X-ray-diffractometry and transmission electron microscopy (TEM). The glass transition and crystallization temperatures were measured by a differential scanning calorimetry (DSC) at a scanning rate of 0.67 and 0.33 K/s. The time-temperature-transformation ($T-T$) diagram of the crystallization was constructed by measuring the time up to the onset of an exothermic reaction on the isothermal DSC curve. The viscosity was measured using a thermomechanical analyzer (TMA) under a tensile stress of 3 MPa at a heating rate of 0.33 K/s. The ductile-proof temperature, namely, the maximum annealing temperature for maintaining good ductility (bending by 180 degrees) was evaluated by bending tests of the melt-spun ribbon annealed for 60 s at various temperatures using the DSC equipment. The tensile tests were conducted using an Instron-type tensile test machine at a constant crosshead velocity over a wide range of temperatures (below, through, and above the glass transition temperature). Strain rates in the range of 1.67×10^{-4} to $5.0 \times 10^{-1} \text{ s}^{-1}$ were used. The test pieces were

*IMR, Report No. 2068

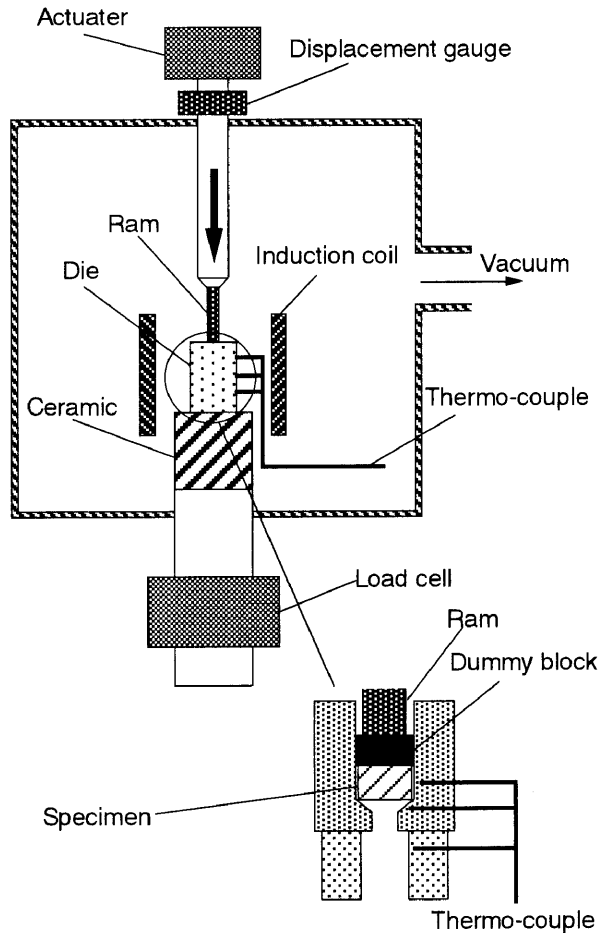


Figure 1. Schematic illustration of an extrusion equipment used in the present study.

produced by bonding the metallic glass ribbon on the ceramic holders with a ceramic cement for achieving the homogeneous and rapid heating. The gauge length was 10 mm. The tensile tests were started after keeping for 200 s from the time when the thermocouple located close to the sample indicated the testing temperature.

$Zr_{65}Al_{10}Ni_{10}Cu_{15}$ bulk metallic glasses used for the investigation of the workability were produced using arc-melting apparatus where the prealloyed ingot of 10 g was arc-melted repeatedly and then rapidly solidified on the water-cooled copper hearth in an argon gas atmosphere. The bulk $Zr_{65}Al_{10}Ni_{10}Cu_{15}$ metallic glasses for the working were machined from the rapidly solidified ingot into a cylindrical shape with 6.5 mm in diameter and 5.0 mm in height. Figure 1 shows the schematic illustration of the hot-working apparatus. In this equipment, the conditions of temperature, ram speed, ram position and load can be well controlled and monitored using a personal computer¹²⁾. In this study, the extrusion was conducted under a constant ram-speed. The split conical die with a hole of gear shape, which had a extrusion ratio of 5, was used. The sample and the die assembly were heated quickly using high-frequency induction coil in a vacuum. The amorphicity of the extruded samples was examined by X-ray diffractometry and DSC. The appearance was also

investigated by optical microscopy. Tensile tests of the extruded bulk metallic glass was conducted using an Instron testing machine at room temperature and at a strain rate of $5.0 \times 10^{-4} s^{-1}$.

3. Results

3.1. Glass transition and crystallization behavior

Figure 2 shows the DSC curve of the metallic glass at a scanning rate of 0.67 K/s. The glass transition temperature T_g , crystallization temperature T_x and supercooled liquid region $\Delta T_x (= T_x - T_g)$ are 652 K, 757 K and 105 K, respectively. The crystallization behavior of glassy alloys is usually dependent on heating time, heating rate and temperature. At the heating rate of 0.33 K/s, the T_x is 735 K, resulting in ΔT_x of 83 K. Figure 3 shows the time-temperature-transformation diagram of the $Zr_{65}Al_{10}Ni_{10}Cu_{15}$ metallic glass. For example, the duration for retaining the glassy phase without decomposition at the temperature (696K) where the viscosity shows the minimum value ($T_{\eta_{min}}$) is 1700 s. The maximum temperature for maintaining good ductility (bending by 180 degrees) in the annealed glassy ribbon for 60 s is 728 K. This ductile-proof temperature is taken as the upper limit of processing temperature to avoid embrittlement. As above described, the glassy alloy has a wide time window for processing in the supercooled liquid region, as compared with the other glassy alloys.

3.2. Deformation behavior

3.2.1. Stress-strain curves

Figure 4 (a) shows the temperature dependence of the stress-strain curve at a strain rate of $5.0 \times 10^{-4} s^{-1}$ for the $Zr_{65}Al_{10}Ni_{10}Cu_{15}$ glassy ribbon. The deformation

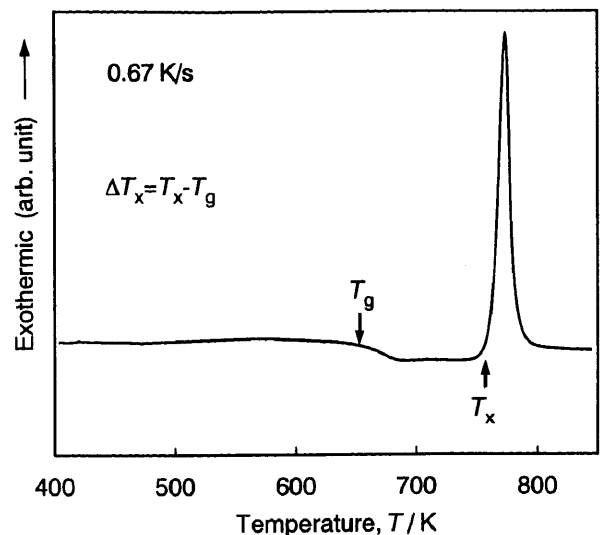


Figure 2. Differential scanning calorimetric (DSC) curve of $Zr_{65}Al_{10}Ni_{10}Cu_{15}$ metallic glass at a heating rate of 0.67 K/s. The T_g and T_x represent the glass transition temperature and the crystallization temperature, respectively.

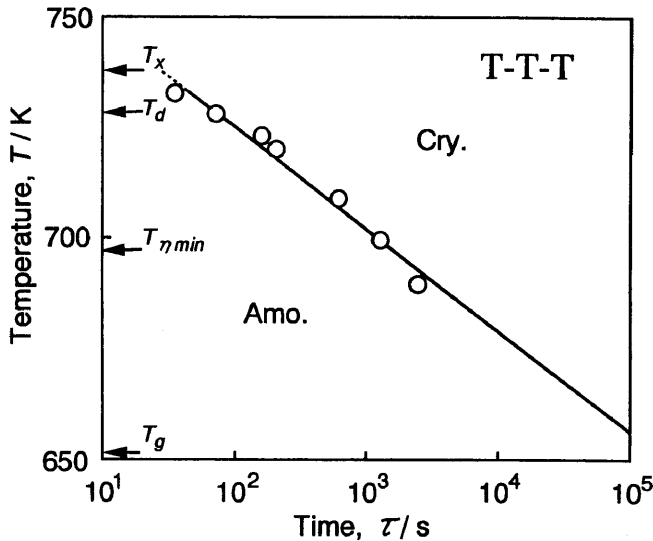


Figure 3. Time-temperature-transformation (*T-T-T*) diagram for the onset of the crystallization in $Zr_{65}Al_{10}Ni_{10}Cu_{15}$ glassy alloy.

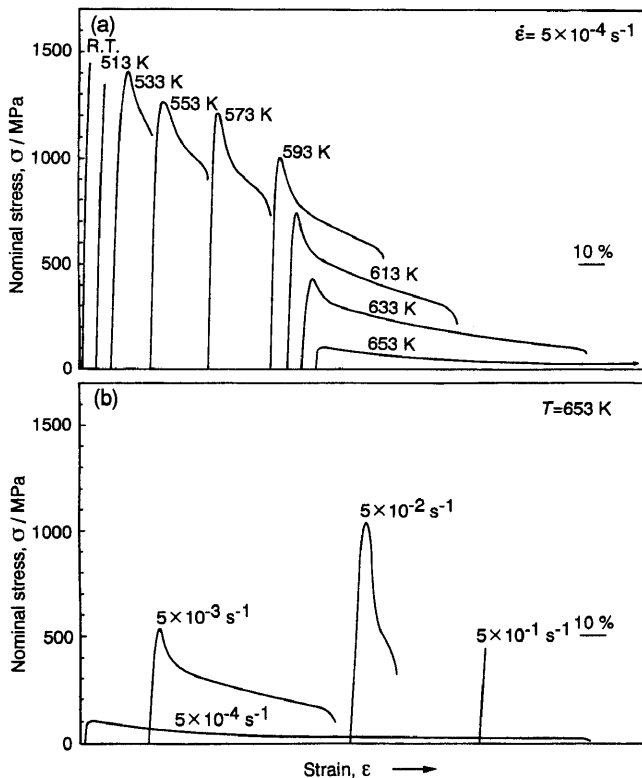


Figure 4. Changes in the stress-strain curves as a function of testing temperature at $5.0 \times 10^{-4} s^{-1}$ (a) and as a function of strain rate at 653 K (b) for $Zr_{65}Al_{10}Ni_{10}Cu_{15}$ glassy alloy.

mode changes from inhomogeneous type to homogeneous one at around 533 K. In the homogeneous deformation regime, the strength decreases and the elongation increases with increasing temperature. Figure 4 (b) shows the strain-rate dependence of the stress-

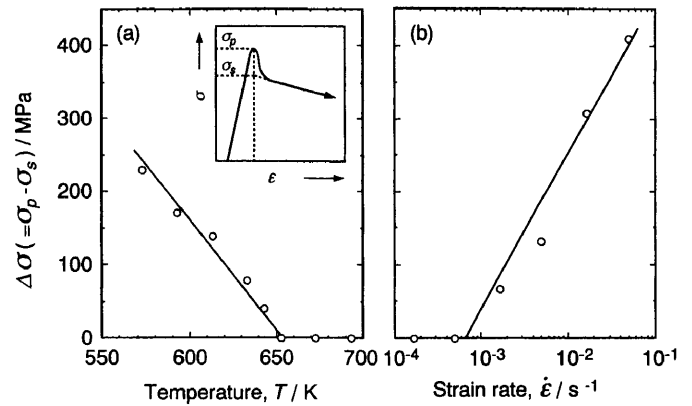


Figure 5. Changes in the stress overshoot $\Delta\sigma$, which is the difference between the peak stress σ_p and the stable stress σ_s as shown in the inset, as a function of testing temperature at a strain rate of $5.0 \times 10^{-4} s^{-1}$ (a), and as a function of strain rate at 653 K (b) for $Zr_{65}Al_{10}Ni_{10}Cu_{15}$ glassy alloy.

strain curve at a temperature of 653 K which is close to T_g (652 K). The strength increases and the elongation decreases with strain rate. The homogeneous mode of deformation, moreover, changes to inhomogeneous type at a higher strain rate ($5.0 \times 10^{-1} s^{-1}$). We define the maximum stress σ_m as yield stress σ_p , and the difference between the yield stress σ_p and the stable flow stress σ_s as a stress overshoot $\Delta\sigma$ for homogeneous deformation, as shown in the inset of Fig. 4.

One should not overlook that the deformation in homogeneous region begins to yield with a maxima, namely, a stress overshoot, and then transfers to stable flow. The height of the stress overshoot $\Delta\sigma$ decreases with increasing temperature and decreasing strain rate as shown in Fig. 5. Little attention has been given to the stress overshoot, although such stress-strain curves were observed in some metallic glasses such as Pd-, Mg- and La-based alloys¹³⁻¹⁵. The stress overshoot seems to be unexplainable by a change in sample shape such as necking because the phenomenon is also observed under compressive loading. The dislocation theory applied to crystalline materials is, moreover, inapplicable to the glassy alloys. The stress overshoot can, however, be explained by viscoelastic properties including relaxation¹⁶.

3. 2. 2. Deformation mode and tensile strength

Figure 6 shows the temperature dependence of the deformation mode and tensile strength for the $Zr_{65}Al_{10}Ni_{10}Cu_{15}$ glassy ribbon. With increasing temperature, the deformation mode changes from the inhomogeneous type to homogeneous one at a certain temperature. This critical temperature depends upon the strain rate. In the inhomogeneous regime, the strength has very weak temperature dependence and strong strain rate sensitivity. On the other hand, the strength in the homogeneous region depends on both the temperature

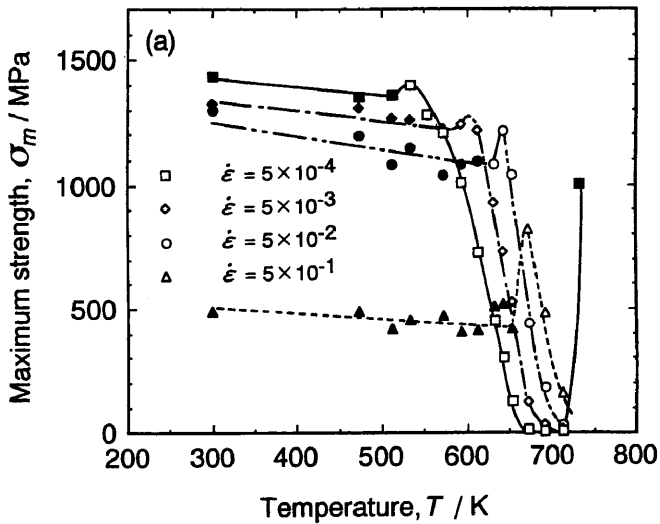


Figure 6. Testing temperature dependence of the maximum tensile strength for $Zr_{65}Al_{10}Ni_{10}Cu_{15}$ glassy alloy. The open and solid symbols represent for the alloys to be deformed homogeneously and inhomogeneously, respectively.

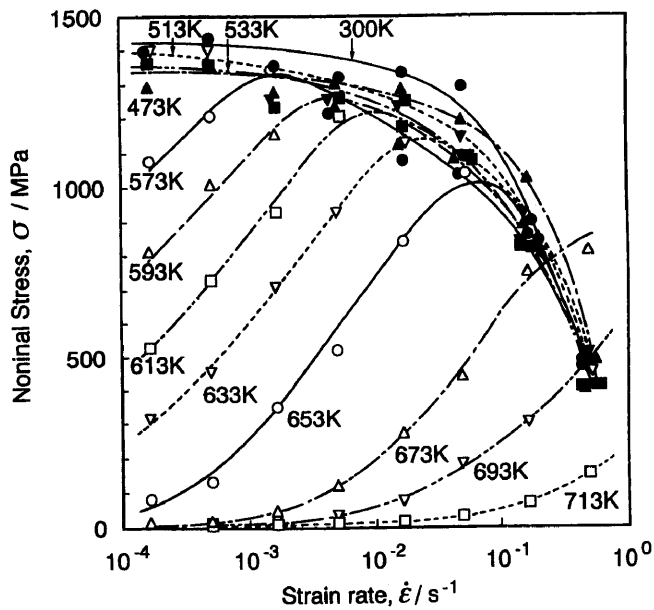


Figure 7. Strain rate dependence of the maximum tensile strength for $Zr_{65}Al_{10}Ni_{10}Cu_{15}$ glassy alloy. The open and solid symbols represent for the alloys to be deformed homogeneously and inhomogeneously, respectively.

and strain rate. The strength reveals a peak at first stage when the deformation mode changes to homogeneous type, and then decreases suddenly with increasing temperature. At higher strain rates, this tendency is shifted towards higher temperatures and the peak in strength becomes higher. The peak at first stage seems to be closely related to the stress overshoot.

Figure 7 shows the strain rate dependence of the maximum strength for the $Zr_{65}Al_{10}Ni_{10}Cu_{15}$ glassy alloy.

As the strain rate increases, the maximum strength increases in the homogeneous mode and then the deformation mode changes to inhomogeneous type, and the maximum strength decreases in the inhomogeneous mode. The critical temperature, where the deformation mode changes from homogeneous type to inhomogeneous one, is shifted towards higher strain rates with increasing temperature. The homogeneous deformation mode in the stable supercooled liquid region above 673 K, however, remains unchanged as it is seen even at higher strain rate of $0.5 s^{-1}$. In the two deformation modes there are distinct differences in the strain rate and temperature dependence of the maximum strength. In the inhomogeneous region, the strength has very weak temperature dependence and strong strain rate sensitivity, resulting in an identical strength within the accuracy of 20 % at each strain rate. The strain rate dependence of the strength is slight at the strain rates up to $5.0 \times 10^{-2} s^{-1}$ and significant in the higher strain rate range. On the other hand, in the homogeneous region the strength is very sensitive to both the temperature and strain rate. The strength decreases with increasing temperature and decreasing strain rate.

3. 2. 3. Strain rate sensitivity (*m* value)

Figure 8 shows the relationship between the flow stress and strain rate. The curves exhibit a sigmoidal shape and shift towards higher strain rates with increasing temperature. The flow stress increases rapidly in the intermediate-strain rates region. It is clear that the supercooled liquid capable to deform at high strain rate above $1 \times 10^{-2} s^{-1}$ under flow stress below 100 MPa. On the contrary, higher stress above 200 MPa is necessary to

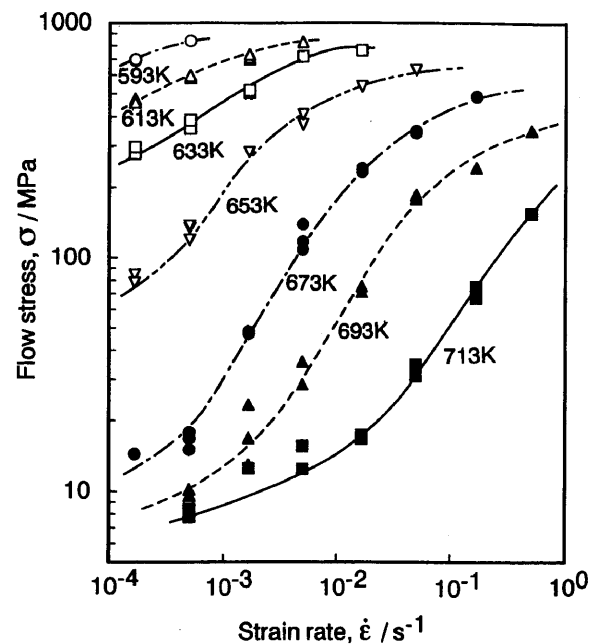


Figure 8. Strain rate dependence of the flow stress at various temperatures for $Zr_{65}Al_{10}Ni_{10}Cu_{15}$ metallic glass.

homogeneously deform the glassy solid even at a low strain rate of 10^{-4} s^{-1} .

Strain rate sensitivity exponent, namely, m value is usually represented by the equation (1).

$$m = \Delta \log \sigma / \Delta \log \dot{\epsilon} \quad (1)$$

Figure 9 shows the strain rate dependence of the m value at various temperatures. The metallic glass exhibits a peak in the m value at a certain strain rate. As temperature increases, the curve shifts towards higher strain rates. In the glassy solid, the m value is weakly dependent on the strain rate and exhibits less than 0.3. On the contrary, the supercooled liquid has strong strain rate dependence of the m value and reveals higher m values above 0.3. One should overlook that the m value in the stable supercooled liquid reaches to as high as 0.8 even at high strain rates above $1.0 \times 10^{-2} \text{ s}^{-1}$.

3. 2. 4. Elongation to failure

Figure 10 shows the strain rate dependence of the elongation to failure at various temperatures. The glassy alloy is significantly elongated in the homogeneous deformation region in which the elongation is dependent on both the temperature and strain rate. As the strain rate increases, the elongation increases, reaches a peak and then decreases. The stable glassy solid exhibits a broad peak in the elongation at a strain rate of about $5.0 \times 10^{-4} \text{ s}^{-1}$, where the elongation is less than 100%. On the other hand, the supercooled liquid has a strong strain rate sensitivity of the elongation and exhibits large elongation of more than 200%. The peak in the elongation of the supercooled liquid is shifted towards higher strain rates with increasing temperature. A large

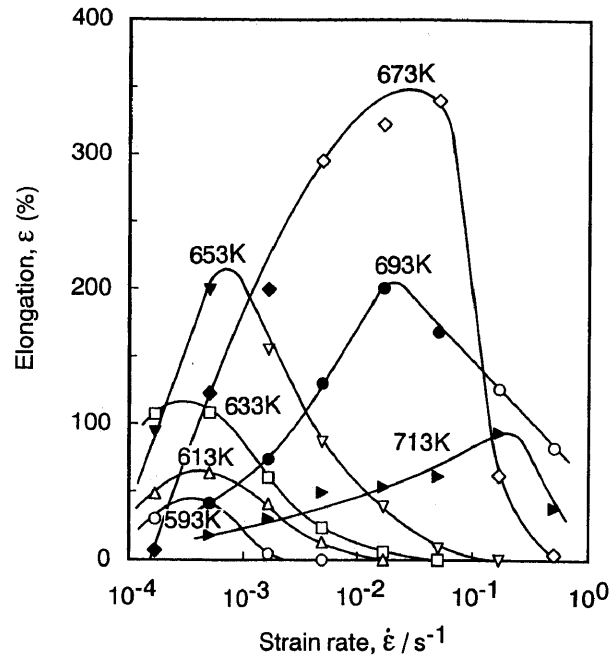


Figure 10. Changes in the elongation to failure at various temperatures as a function of strain rate for $\text{Zr}_{65}\text{Al}_{10}\text{Ni}_{10}\text{Cu}_{15}$ metallic glass. The samples indicated with the open and solid symbols exhibit the ductile and brittle nature, respectively, at room-temperature after testing.

elongation of 300% is obtained even at high strain rates above $5.0 \times 10^{-3} \text{ s}^{-1}$. The maximum elongation achieved in this study was 340% at 673 K and $5.0 \times 10^{-2} \text{ s}^{-1}$. The samples represented with a solid symbol in Fig. 10 have brittle nature at room temperature after testing. This result reveals that the testing at lower strain rates and at higher temperatures leads to the embrittlement. The duration of retaining the glassy phase without decomposition becomes shorter at higher temperatures, as shown in the T - T - T diagram (Fig. 3). Moreover, it takes longer time to elongate the samples prior to failure at lower strain rate. The embrittlement, therefore, seems to be due to the crystallization during tensile tests. On the contrary, the samples indicated with an open symbol exhibit ductile nature and original strength at room temperature. It is clear that the supercooled liquid of the metallic glass enables to be deformed at high strain rates without losing the original mechanical properties.

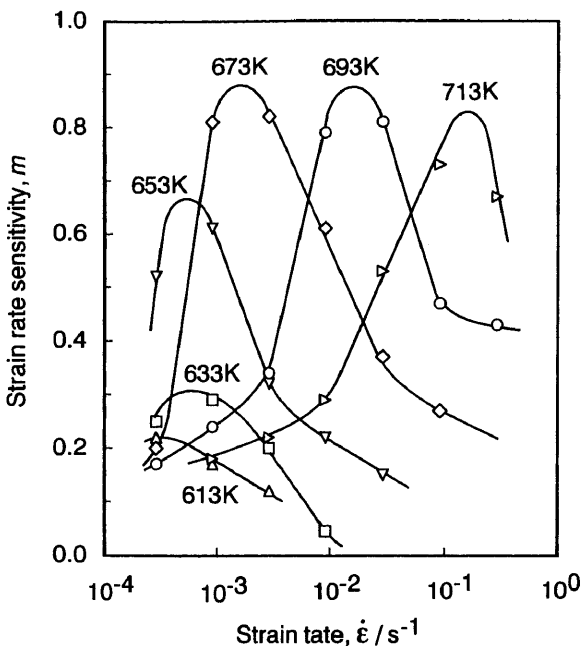


Figure 9. Strain rate dependence of the m value at various testing temperatures for $\text{Zr}_{65}\text{Al}_{10}\text{Ni}_{10}\text{Cu}_{15}$ metallic glass.

3. 3. Working of the metallic glass through extrusion

On the basis of the above-described results, we investigated the workability of the bulk $\text{Zr}_{65}\text{Al}_{10}\text{Ni}_{10}\text{Cu}_{15}$ metallic glass through extrusion at the supercooled liquid state. The extrusion of the metallic glass was carried out using a conical die with a gear-shape hole. Figure 11 shows the metallic glass extruded successfully at 693 K and a ram speed of $3.5 \times 10^{-2} \text{ mm/s}$ under an extrusion pressure of 780 MPa. The outer edge of the extruded glass appears to be very sharp, indicating that the working of the supercooled liquid makes it possible to produce net-shaped fine and precise glassy articles

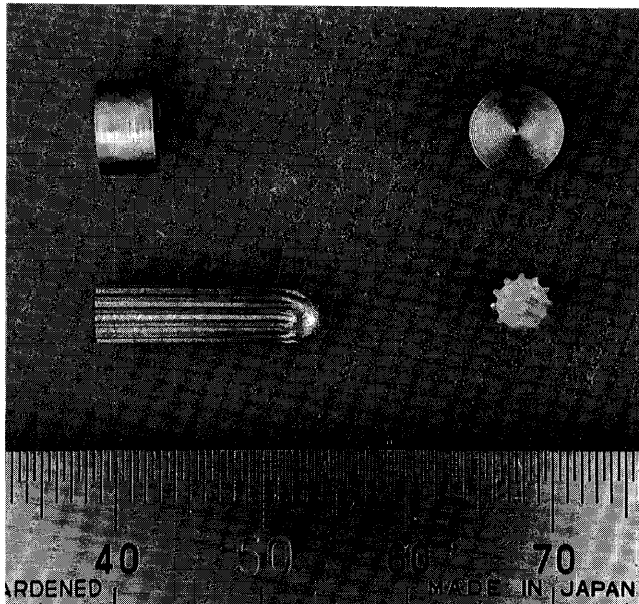


Figure 11. Complex-shaped $Zr_{65}Al_{10}Ni_{10}Cu_{15}$ metallic glasses product extruded at 693 K and $3.5 \times 10^{-2} \text{ mm s}^{-1}$ through the conical die with a gear-shape hole.

with complex shapes. The DSC curve and the X-ray diffraction pattern of the extruded alloy are shown in Figs. 12 and 13, respectively. No peak corresponding to a crystalline phase is observed in the X-ray diffraction pattern for the extruded alloy. Furthermore, no appreciable difference in the DSC curves between the as-cast and as-extruded samples is seen. This suggests that the glassy phase is retained even after extrusion. The metallic glass extruded at 693 K, $3.5 \times 10^{-2} \text{ mm/s}$ and an extrusion ratio of 5 using a conical die with a hole of circle shape has a tensile strength of 1560 MPa, which is similar to that of the casted bulk glassy alloy (1570 MPa) and melt-spun glassy ribbon (1440 MPa)¹⁴. The fracture takes place along the maximum shear plane which is inclined by about 45 degrees to the direction of tensile load. The fracture surface consists mainly of a well-developed vein pattern, which is a typical fracture pattern for glassy alloys with good bending ductility. Thus, the worked metallic glasses appear to maintain good ductility without embrittlement. These results indicate that the metallic glasses are able to be worked with retaining the original mechanical properties.

4. Discussion

We now discuss the features of the deformation from the view point of superplasticity. The most important mechanical characteristic of a superplastic material is its high m value^{17,18}. The presence of a neck in a material subjected to tensile straining leads to a locally high strain rate, leading to a sharp increase in the flow stress within the necked region for materials with a high value of m . Hence the neck undergoes strain rate hardening inhibits its further development. Thus, a high

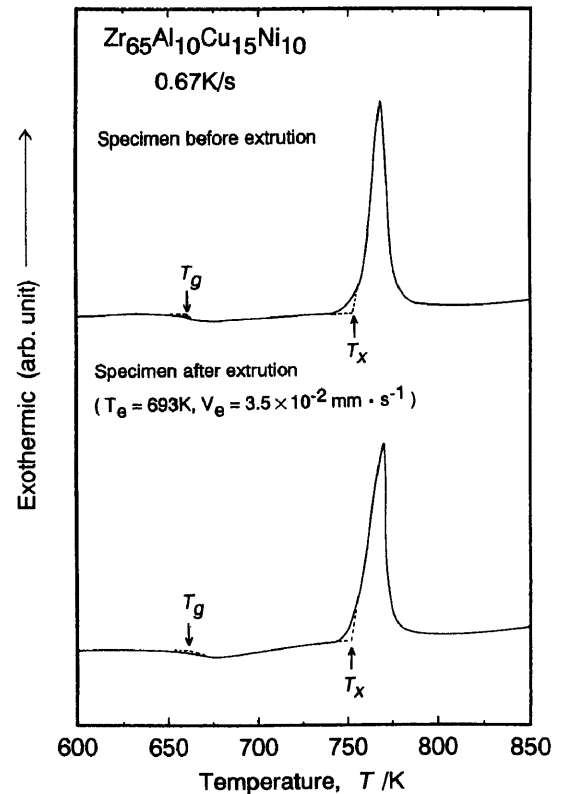


Figure 12. DSC curves of $Zr_{65}Al_{10}Ni_{10}Cu_{15}$ metallic glasses in the as-casted and as-extruded states. The product was extruded at 673 K and $3.5 \times 10^{-2} \text{ mm s}^{-1}$.

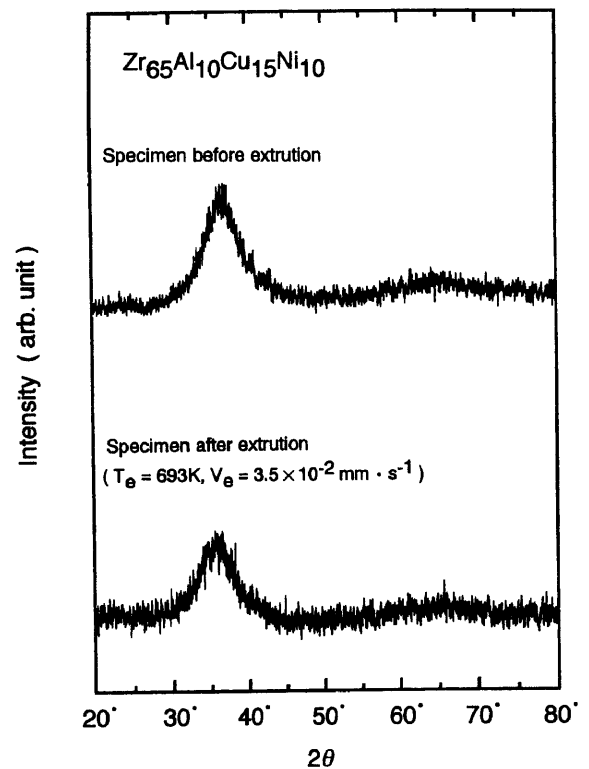


Figure 13. X-ray diffraction patterns of $Zr_{65}Al_{10}Ni_{10}Cu_{15}$ metallic glasses in the as-casted and as-extruded states. The product was extruded at 673 K and $3.5 \times 10^{-2} \text{ mm s}^{-1}$.

strain rate sensitivity confers a high resistance to neck development and results in high tensile elongations to failure.

Superplastic materials usually exhibit a large elongation to failure in excess of 200 % for deformation in uniaxial tension, and high m values of more than 0.3, and sigmoidal shape in $\log \sigma$ vs $\log \dot{\epsilon}$ plots¹⁸⁾. Especially, the superplasticity observed at high strain rates of more than $1.0 \times 10^{-2} \text{ s}^{-1}$ is termed "high-strain-rate superplasticity". In the present work, the supercooled liquid of $\text{Zr}_{65}\text{Al}_{10}\text{Ni}_{10}\text{Cu}_{15}$ metallic glass exhibited a sigmoidal shape in $\log \sigma$ vs $\log \dot{\epsilon}$ plots, and large m values in the range of 0.3 to 0.8, and large elongations more than 200 % at higher strain rates above $1.0 \times 10^{-2} \text{ s}^{-1}$. These are the same deformation behavior as the other high-strain-rate superplastic materials. Hence, similar techniques to those developed for superplastic materials are expected to be applicable to the work of the metallic glass, being of considerably significant from industrial view point. Although the word of "superplasticity" is defined to be applicable to only polycrystalline solids, we can say that the glassy alloys with a wide supercooled liquid region is a new type of high-strain-rate superplastic materials.

It has been reported that La-Al-Ni metallic glass exhibited a high m value of about 1.0 in a supercooled liquid under lower stresses and lower strain rates¹⁰⁾. The above-described features of workability in the $\text{Zr}_{65}\text{Al}_{10}\text{Ni}_{10}\text{Cu}_{15}$ metallic glass seem to be in good agreement with the previous data, and hence are applicable to the other glassy alloys with a wide supercooled liquid region. Furthermore, the high processability is available for the fabrication of large-scale bulk metallic glasses by consolidation of glassy powders. Consequently, interest in the viscous flow deformation of the supercooled liquid in the metallic glasses and its commercial potential as the basis of an important forming process are expected to increase significantly.

5. Conclusions

We have investigated the deformation behavior of the $\text{Zr}_{65}\text{Al}_{10}\text{Ni}_{10}\text{Cu}_{15}$ glassy alloy with a wide supercooled liquid region. The results obtained are summarized as follows.

(1) The deformation mode is dependent on both strain rate and temperature in the temperature range below T_g . The higher temperature and lower strain rate revealed homogeneous deformation. The alloy in the supercooled liquid state was, moreover, deformed homogeneously even at high strain rates above 0.5 s^{-1} .

(2) The strength is dependent on strain rate and independent of temperature in the inhomogeneous deformation mode, and is very sensitive to both strain rate and temperature in the homogeneous deformation mode. The strength in the homogeneous deformation region becomes lower at higher temperature and lower

strain rate.

(3) The stress-strain curves in the homogeneous deformation were accompanied by a stress overshoot whose height increases with decreasing temperature and increasing strain rate.

(4) The supercooled liquid of the metallic glass exhibited similar deformation behavior to the other high-strain-rate superplastic materials. The plot of $\log \sigma$ versus $\log \dot{\epsilon}$ revealed a sigmoidal shape. The supercooled liquid above the glass transition temperature had the m values from 0.3 to 0.8 and the elongation more than 200 %, respectively.

(5) Complex-shaped components with original strength and ductility and glassy phase was produced by extrusion of the bulk metallic glass using the superplastic-like deformation of the supercooled liquid.

- 1) T. Masumoto and R. Maddin: *Acta Met.* 19 (1971) 725.
- 2) F. Spaepen and A. I. Taub: *Amorphous Metallic Alloys*, ed. F. E. Luborsky (Butterworths, London, 1983) p. 231.
- 3) A. Inoue, T. Zhang and T. Masumoto: *Mater. Trans. JIM* 31 (1990) 17.
- 4) A. Inoue, T. Zhang and T. Masumoto: *Mater. Trans. JIM* 31 (1990) 17.
- 5) A. Inoue, T. Zhang and T. Masumoto: *Mater. Trans. JIM* 36 (1995) 391.
- 6) A. Peker and W. L. Johnson: *Appl. Phys. Lett.* 63 (1993) 2342.
- 7) A. Inoue and J. S. Gook: *Mater. Trans. JIM* 36 (1995) 1180.
- 8) Y. Kawamura, H. Kato, A. Inoue and T. Masumoto: *Appl. Phys. Lett.* 67 (1995) 2008.
- 9) H. Kato, Y. Kawamura, A. Inoue and T. Masumoto: *Mater. Trans. JIM* 37 (1996), 70.
- 10) Y. Saotome and A. Inoue: *Proc. 7th IEEE Workshop on Micro Electro Mechanical Systems*, (1994) 343.
- 11) Y. Kawamura, T. Shibata, A. Inoue and T. Masumoto: *Appl. Phys. Lett.* 69 (1996) 1208.
- 12) A. Inoue, Y. Kawamura, T. Shibata and K. Sasamori: *Mater. Trans. JIM* 37 (1996) 713..
- 13) Y. Kawamura, A. Inoue and T. Masumoto: *J. Japan Soc. Powder and Powder Metallurgy* 38 (1991) 110.
- 14) A. Inoue, T. Nakamura, N. Nishiyama and T. Masumoto: *Mater. Trans. JIM* 33 (1992) 937.
- 15) A. Inoue, T. Zhang and T. Masumoto: *Mater. Trans. JIM* 31 (1990) 425.
- 16) B. Maxwell and M. Nguyen: *Polym. Eng. Sci.* 19 (1979) 1140.
- 17) O. D. Sherby and J. Wadsworth: *Prog. Mater. Sci.* 33 (1989) 169.
- 18) J. Pilling and N. Ridley: *Superplasticity in Crystalline Solids* (The Institute of Metals, London, 1989).